T-MQM: Testbed based Multi-metric Quality Measurement of Sensor Deployment for Precision Agriculture-A Case Study

Omprakash Kaiwartya, *Member IEEE*, Abdul Hanan Abdullah, *Member IEEE*, Yue Cao, *Member IEEE*, Ram Shringar Raw, Sushil Kumar, *Member IEEE*, Xiulei Liu, Rajiv Ratn Shah, *Student Member IEEE*

***Abstract*— Efficient sensor deployment is one of primary requirements of precision agriculture use case of Wireless Sensor Networks (WSNs) to provide qualitative and optimal coverage and connectivity. The application-based performance variations of the geometrical-model-based sensor deployment patterns restricts the generalization of a specific deployment pattern for all applications. Further, single or double metrics based evaluation of the deployment patterns focusing on theoretical or simulation aspects can be attributed to the difference in performance of real applications and the reported performance in literature. In this context, this paper proposes a Testbed based Multi-metric Quality Measurement (T-MQM) of sensor deployment for precision agriculture use case of WSNs. Specifically, seven metrics are derived for qualitative measurement of sensor deployment patterns for precision agriculture. The seven metrics are quantified for four sensor deployment patterns to measure the quality of coverage and connectivity. Analytical and simulation based evaluations of the measurements are validated through testbed experiment based evaluations which are carried out in 'INDRIYA' WSNs testbed. Towards realistic research impact, the investigative evaluation of the geometrical-model-based deployment patterns presented in this article could be useful for practitioners and researchers in developing performance guaranteed applications for precision agriculture and novel coverage and connectivity models for deployment patterns.**

***Index Terms*— Precision agriculture, Testbed, WSNs, Deployment**

I. Introduction

Application of Wireless Sensor Networks (WSNs) is expanding enormously due to the inclusion of new areas day by day. Few examples of the application area include environmental monitoring, agricultural monitoring, on-road traffic monitoring, vehicular communication, healthcare, home automation and indoor energy conservation, and warfare [1-3].

The research is supported by Ministry of Education Malaysia (MOE) and conducted in collaboration with Research Management Center (RMC) at University Teknologi Malaysia under VOT NUMBER: RJ130000.7828.4F708

O. Kaiwartya, A.H. Abdullah, are with the Faculty of Computing, Universiti Teknologi Malaysia (UTM), Johor Bahru, 81310, Malaysia. Email: omprakash@utm.my; hanan@utm.my

Y. Cao (Corresponding Author) is with the Department of Computer Science and Digital Technologies, Northumbria University, Newcastle upon Tyne, NE1 8ST, UK. Email: yue.cao@northumbria.ac.uk

R. S. Raw is with the Department of Computer Science, Indira Gandhi National Tribal University, M.P., India, 484886, Email: rsrao08@yahoo.in

S. Kumar is with the School of Computer & Systems Sciences, Jawaharlal Nehru University, New Delhi, India, 110067. Email: skdohare@mail.jnu.ac.in

Xiulei Liu is with the Computer School, Beijing Information Science and Technology University, Beijing, 10010, China. Email: xiuleiliu@hotmail.com

R. R. Shah is with the School of Computing, National University of Singapore (NUS), Singapore, 117417. Email: rajiv@comp.nus.edu.sg

In any application of WSNs, sensor deployment is one of the most important and critical issue since it is directly related to the cost and performance of the applications. A better sensor deployment strategy not only reduces the redundancy of sensors subsequently minimizing the cost of the network, but also extends the lifetime of the network [4].

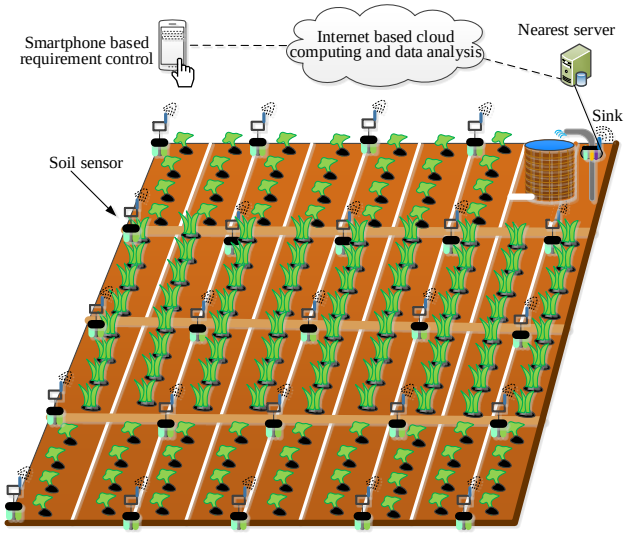

Fig. 1. Precision agriculture use case of WSNs

The deployment patterns followed in planned sensor deployment have significant impact on the performance of wireless sensor networks [5]. Therefore, these patterns are considerably important for the applications of sensors in regular terrain non-hostile environment where planned sensor deployment is followed. Precision agriculture is one of the promising use case of planed sensor deployment of WSNs in regular terrain non-hostile environment [6]. Recently, precision agriculture using WSNs has witnessed significant attention from industries as well as academia due to the huge potential to increase per hectare production in agriculture by efficient and automated nutrition requirement control in forming [7]. Various patterns for planned sensor deployment have been suggested for the applications in regular terrain non-hostile environment; e.g., precision agriculture, which are based on geometrical models including square, rhombus, pentagon and hexagon [8]. An application of square deployment pattern in precision agriculture is depicted in Fig. 1 in which soil sensors are utilized to remotely monitor and control the nutrition requirements of plants in forming.

The geometrical model based deployment patterns followed in planned sensor deployment have significant impact on the

overall performance of the applications of wireless sensor networks [9]. Due to the different physical characteristics of these geometrical models, considerable variations have been observed on performance of the deployment patterns based on these geometrical models in different kinds of applications [10]. The application-based performance variations restricts the generalization of the performance of a particular deployment pattern for all kinds of applications [11]. Therefore, qualitative measurements of these geometrical model based deployment patterns for precision agriculture use case of WSNs need to be investigated considering the early stage development in precision agriculture use case of WSNs [9, 12]. Further, most of these geometrical model-based deployment patterns have been evaluated using single [13-16] or double [17-20] metrics of coverage and connectivity. In real applications, performance of these geometrical model-based deployment patterns are quite different and far away from the reported performance in literature which are based on evaluations considering single or double metrics of coverage and connectivity [21]. Insufficient number of metrics for measuring coverage and connectivity is a cause of concern in terms of monitoring quality [22]. The inter-dependency of metrics have not been investigated which is also one of the main reasons for the quite deviation in the performance of applications from the reported performance [23]. It is also highlighted that majority of the previous works on quality measurement in WSNs pay attention on theoretical or simulation based evaluation, whereas this paper focuses on testbed experiment based evaluation.

In this context, this paper proposes Testbed-based Multi-metric Quality Measurement (T-MQM) to evaluate sensor deployment patterns in terms of offered quality of coverage and connectivity for precision agriculture use case of WSNs. The key contributions of the paper are as follows.

1) The derivation of seven metrics for measuring quality of coverage and connectivity which are correlated with each other for effectively analyzing the impact of inter-dependency of metrics on the performance of deployment patterns.
2) The quantification of seven metrics for four sensor deployment patterns of precision agriculture use case to measure the quality of coverage and connectivity.
3) The analytical and simulation evaluations of the quality of coverage and connectivity measurements using mathematical analysis and Network Simulator (NS-2); respectively.
4) The testbed experiment based assessment using 'INDRIYA' wireless sensor network testbed at School of Computing, National University of Singapore (NUS) [24] to validate the analytical and simulation evaluations.

The rest of the paper is organized in following sections. Section II qualitatively reviews coverage and connectivity measurements in wireless sensor networks by categorizing the theme into single, double and multiple metrics based measurements and points out the research gap in deployment measurement for precision agriculture. Section III presents derivation of the seven metrics and measurement of quality of coverage and connectivity for four deployment patterns by quantifying the seven metrics. Section IV discusses the analytical, simulation and testbed based evaluations of the measurement of deployment patterns. Section V concludes this paper with some future directions of research in the theme.

II. Related Work

In this section, a qualitative review on coverage and connectivity measurements of sensor deployment in wireless sensor networks is presented, by classifying the theme into three categories including single, double and multi-metric based measurement. The contribution area of the paper; i.e., precision agriculture using WSNs, is revisited to precisely point out the research gap in deployment measurement for precision agriculture use case.

A. Single Metric based Measurement

Analysis of quality of deployment in Surveillance Wireless Sensor Networks (SWSNs) has been performed using probabilistic models with detection ratio as a single metric for measurement [13]. Authors have suggested the usage of image segmentation algorithm for reducing the impact of obstacles in deployment strategies. The number of sensor requirement has been studied and analyzed experimentally considering the probability of detecting intrusion and time taken for detection. Mathematical model for measuring deployment quality and analytical analysis of the iso-sensing graph based approach has not been provided in this surveillance analysis. Various deployment patterns have been explored to obtain Optimal Deployment Patterns (ODP) for providing full coverage and k-connectivity ($k \leq 6$) using percentage coverage metric [14]. Authors have presented a universal elementary deployment pattern to generate the other optimal deployment patterns considered. The universal deployment pattern is based on hexagon geometry. They have also suggested an approach to prove an optimal pattern for the situation where Voronoi diagram based approach is not suitable. In spite of analyzing regular deployment pattern, overlapped coverage area has not been taken into consideration. Un-even deployment of sensors in the sensing region or error in deployment planning may result into interference in wireless sensor networks.

Impact of Interference in Wireless Communication has been investigated in Fading Environment (IWC-FE) using outage probability metric [15]. Authors have analyzed co-channel interference and derived mathematical functions; i.e. probability density function and cumulative density function for signal-to-noise interference ratio. Although intensity of interference is closely related with physical deployment of sensors yet, the impact of deployment patterns on interference has not been taken into consideration. Regular and Random Deployment patterns have been evaluated in terms of Throughput (RRD-T) metric which is significantly dependent on connectivity metric [16]. Authors have utilized 'slotted ALOHA' as Medium Access Control (MAC) protocol and Rayleigh distribution as fading channel. In particular, authors have mathematically derived average link throughput for three regular deployment patterns; namely square, triangular and hexagonal and compared the performance of these deployment patterns in terms of throughput, transmission efficiency and delivery capacity. Although the analysis has been validated

through numerical simulations yet, verification of the results using network simulator platform is missing.

B. Double Metrics based Measurement

Quality of Connectivity of Regular Topologies (QC-RT) has been evaluated using two metrics; namely, isolation probability and end-to-end connectivity for geometrical deployment patterns [17]. Authors have used probabilistic models to analyze connectivity considering reliability of sensors and fading of channels due to the interferers and multiple channel access. Three different fading models; namely, Rayleigh, Nakagami and Log normal have been used to analyze probabilistic connectivity in terms of node isolation probability and end-to-end network connectivity. The analysis did not consider coverage in spite of the fact that coverage and connectivity should be studied together due to their companion nature. Minimum number of sensors required for retaining a sensor network functioning with desired level of coverage and connectivity has been estimated using distance and degree metrics of graph theory in Connectivity Coverage and Power Consumption (CCPC) [18]. Authors have suggested a network management protocol for equalizing the remaining energy among all the sensors by switching off appropriate sensors in time slots while maintaining the desired coverage and connectivity. Presence of obstacles has not been taken into consideration in spite of analyzing random wireless sensor networks which are mostly deployed in hostile environment where presence of obstacles is un-avoidable.

Two deployment strategies; namely, Expected-area Coverage Deployment (ECD) and Boundary Assistant Deployment (BOAD) have been suggested and evaluated using deployment quality and deployment error metrics for providing guaranteed coverage in wireless sensor networks [19]. Authors have addressed the problem of overestimation of coverage through their deployment strategies. Although random deployment has been considered yet, the presence of obstacles in the field of interest has not been realized. Uncertainty Aware Deployment Technique (UADT) has been evaluated using detection probability and connectivity percentage in mixed wireless sensor networks [20]. In particular, authors have suggested a deployment approach which discovers coverage holes by computing joint detection probability and moves the appropriate mobile sensors into coverage holes using bipartite graph based approach. Uncertainty aware deployment approach assumes that only static sensors are unreliable but the reliability of movable sensors has not been taken into account.

C. Multi-Metrics based Measurement

The multi-metric measurement of coverage and connectivity in WSNs have not been explored accountably for the applications of WSNs in regular terrain non-hostile environment. Some of the following investigations are restricted to either for a specific application which could not be generalized, or for particular type of WSNs with theoretical or simulation perspective. Coverage and connectivity have been evaluated using three metrics; namely, probability of instantaneous event detection, probability of delayed event capture and probability of communication in Duty-Cycled partitioned synchronous Wireless Sensor Networks (DC-WSNs) [25]. The probabilistic models of these metrics have been derived for both synchronous and asynchronous networks. The impact of ratio of duty time and time interval on the performance of these metrics have been explored using mathematical and analytical analysis. Although the optimization of network performance in partitioned synchronous network is a challenging task considering the cooperation requirements among sensors yet, the applicability of the network is minimal due to the synchronization constraints. For bridge monitoring applications, sensor deployment has been evaluated using the metrics including model strain energy index, modal assurance criterion and modal participant factor [26]. Specifically, an optimal sensors placement method has been presented by optimizing multiple performance metrics and resources. There are two major operational steps in the method. Firstly, modal energy index of randomly deployed sensor's locations are enhanced using Modal Strain Energy (MSE) as initial assignment of sensors on the bridge. Secondly, Adapted Genetic Algorithm (AGA) is developed using root mean square based fitness function for optimizing both number of sensors and their locations. No pattern is followed in the evaluation therefore, generalization of the measurement is not possible.

D. The Contribution Area-Precision Agriculture

The applicability of the findings of measurement of the deployment strategies in which any geometrical patterns are not followed, is lesser in other applications in regular terrain non-hostile environment; e.g., precision agriculture. Readers are advised to go through the article [27] to explore more about application-based deployment strategies and related issues. These deployment measurements could not be generalized for other applications of wireless sensor networks in regular terrain non-hostile environment. Precision agriculture is one of the fine use case of WSNs in regular terrain non-hostile environment. Recently, the early stage studies in precision agriculture use case of WSNs has focused on addressing the implementation issues of precision agriculture system. Cluster based WSNs has been considered to optimize IEEE 802.15.4 MAC parameters for precision agriculture [28]. Star topology has been utilized within clusters with a cluster head in each cluster working as getaway for the cluster. The impact of topology change on the performance of the network has not been explored in the MAC parameter optimization. Automated actions based on the intelligence acquired from the perceived, processed and analysed data by sensors is one of the fundamental objectives of precision agriculture which has been investigated as data logger for precision agriculture [29].

A complete system implementation for precision agriculture using WSNs is presented considering two types of sensors; namely, management and normal sensors [30]. Random deployment of normal sensors within monitoring area has been considered therefore, the system lacks the cost and performance optimization using sensor deployment patterns. To address the battery power limitation, and thus replacement or recharging, attached with normal sensor, pluggable Radio Frequency Identification (RFID) based wireless sensor network system for precision agriculture is suggested [31].

The aforementioned recent and early stage investigations on precision agriculture use case of WSNs have considered the design and development of data acquisition system for precision agriculture and claimed that the system is adaptable to different requirements of precision agriculture. From the best of our knowledge, qualitative evaluation of sensor deployment patterns and the impact of deployment patterns on the quality of coverage and connectivity for precision agriculture use case have not been taken into consideration yet [28-31]. It is also observed that majority the works in related literature pay attention on theoretical or simulation based study, whereas this paper focuses on testbed based study.

In this context, Testbed based Multi-metric Quality Measurement (T-MQM) is presented to evaluate geometrical model based sensor deployment patterns for precision agriculture using wireless sensor networks in regular terrain non-hostile environment. Efficient sensor deployment is one of the primary functional module in precision agriculture use case of WSNs. Some of the key requirements of a sensor deployment technique for large scale sensor-based applications; e.g., precision agriculture, include covering the complete sensing field with minimum overlapping coverage area among sensors [32], maintaining quality of connectivity among sensors throughout the networks [33] and reducing network operation cost [34]. To optimize these requirements, the quality of sensor deployment patterns need to be verified through multiple metrics and testbed based measurements rather than relying on single or double metrics and theoretical or simulation based measurements.

III. Testbed based Multi-metric Quality Measurement

In this section, T-MQM is presented for measuring the quality of coverage and connectivity as a real research impact. Firstly, seven metrics are derived to measure the quality of coverage and connectivity of sensor deployment patterns. The metrics include total coverage area, effective coverage area, net effective coverage area, net effective coverage area ratio, total overlapped coverage area, total non-overlapped coverage area, and quality of connectivity. Secondly, the seven metrics are quantified for four sensor deployment patterns including square, rhombus, pentagon and hexagon patterns to measure the quality of coverage and connectivity. The nomenclature used in the design of T-MQM are precisely introduced in Table 1.

Table 1. Nomenclature

Notation	Description
$\mathrm{C}_\mathrm{a}^\mathrm{T}$	Total coverage area
$\mathrm{C}_\mathrm{a}^\mathrm{TO}$	Total overlapped coverage area
$\mathrm{C}_\mathrm{a}^\mathrm{TNO}$	Total non-overlapped coverage area
$\mathrm{C}_\mathrm{a}^\mathrm{E}$	Effective coverage area
C_a^1	Coverage area of a sensor
N	Number of sensors
$\mathrm{C}_\mathrm{a}^\mathrm{NE}$	Net effective coverage area
$\mathrm{C}_\mathrm{a}^\mathrm{IO}$	Individual overlapped coverage area within a sensor
C_a^{NER}	Net effective coverage area ratio
$\mathrm{C}_\mathrm{a}^\mathrm{TNO}$	Total non-overlapped coverage area
$\mathrm{C}_\mathrm{a}^\mathrm{TO}$	Total overlapped coverage area
Q_c	Quality of connectivity
K	Conversion constant
S_i	i^{th}sensor in a sensor deployment pattern
r	Sensing range
t	Transmission range
π	Constant
P	Length of a side of a deployment pattern
d	Distance between two sensors
h	Height of the arcs of the intersection area between two sensors
θ	An angle in a deployment pattern geometry

A. The Metrics

The seven metrics are derived to measure quality of coverage and connectivity of sensor deployment pattern for precision agriculture. The metrics are also applicable for other applications of WSNs in regular terrain non-hostile environment. However, the Squared Error (SE) metric is more relevant for the applications where the requirement of quality of coverage varies on the different sub-regions of a region of interest [35]. This can be attributed to the fact that the SE metric considers the difference between achieved and required detection/miss probabilities on each sub-region before deploying a sensor on any sub-region of a region of interest. In these applications, the constraints in terms of quality of coverage requirement on the different sub-regions, are significant. However, in the context of precision agriculture, different quality of coverage on the sub-regions of a farming region is not considered. The constraints are not attached in case of precision agriculture, and thus, the following metrics are suitable.

1) Total Coverage Area

The total coverage area $\mathrm{C}_\mathrm{a}^\mathrm{T}$ of a sensor deployment pattern in a sensing field is the total area covered by all the sensors. It is the sum of the total overlapped coverage area $\mathrm{C}_\mathrm{a}^\mathrm{TO}$ and total non-overlapped coverage area $\mathrm{C}_\mathrm{a}^\mathrm{TNO}$ among sensing range of the sensors deployed in a sensing field. In terms of precision agriculture, it defines the area of the part of the form where actual forming is practiced. It can be measured as expressed by Eq. (1).

$$C_a^T = \mathrm{C}_\mathrm{a}^\mathrm{TO} + \mathrm{C}_\mathrm{a}^\mathrm{TNO} \quad (1)$$

2) Effective Coverage Area

In a sensing field where N number of sensors are deployed, the effective coverage area $\mathrm{C}_\mathrm{a}^\mathrm{E}$ of a deployment pattern is the ratio of total coverage area and the sum of coverage area of all the individual sensors. In terms of precision agriculture, it defines the area referring to cost effectiveness of deployment pattern. It can be measured as expressed by Eq. (2).

$$C_a^E = \frac{C_a^T}{NC_a^1} = \frac{\mathrm{C}_\mathrm{a}^\mathrm{TO} + \mathrm{C}_\mathrm{a}^\mathrm{TNO}}{N\pi r^2} \quad (2)$$

where, C_a^1 is the coverage area of an individual sensor and r is the sensing range, $C_a^T \leq NC_a^1$ and $\frac{1}{N} \leq C_a^E \leq 1$.

3) Net Effective Coverage Area

In a sensor deployment pattern, the net effective coverage area $\mathrm{C}_\mathrm{a}^\mathrm{NE}$ is the area covered by an individual sensor only. It is the difference between the area C_a^1 covered by an individual sensor and the overlapped coverage area $\mathrm{C}_\mathrm{a}^\mathrm{IO}$ within an individual sensor's coverage area in the deployment pattern. In terms of precision agriculture, it defines the area referring to the unit of coverage in terms of a sensor. It can be measured as expressed by Eq. (3).

$$C_a^{NE} = C_a^1 - \mathrm{C}_\mathrm{a}^\mathrm{IO} = \pi r^2 \left(1 - \frac{\mathrm{C}_\mathrm{a}^\mathrm{IO}}{\pi r^2}\right), \; 0 < C_\mathrm{a}^\mathrm{NE} \leq \pi r^2 \quad (3)$$

4) Net Effective Coverage Area Ratio

In a sensing field where N number of sensors are deployed, the net effective coverage area ratio C_a^{NER} of a deployment

pattern is the ratio of net effective coverage area and an individual sensor's coverage area. In terms of precision agriculture, it defines the unit of qualitative coverage area offered in the return of an asset in terms of an individual sensor's coverage area in a particular deployment patterns. It can be measured as expressed by Eq. (4).

$$C_a^{NER} = \frac{C_a^{NE}}{C_a^1} = \frac{\pi r^2\left(1-\frac{C_a^{IO}}{\pi r^2}\right)}{\pi r^2} = 1 - \frac{C_a^{IO}}{\pi r^2}, 0 < C_a^{NER} \leq 1 \quad (4)$$

5) Total Non-overlapped Coverage Area

The total non-overlapped coverage area C_a^{TNO} of a deployment pattern is the total coverage area covered by individual sensors only in the sensing field. In terms of precision agriculture, it defines the overall area within the form which is qualitatively monitored by geometrically deployed sensors following a particular deployment pattern. It can be measured as expressed by Eq. (5).

$$C_a^{TNO} = NC_a^{NE} = N(\pi r^2 - C_a^{IO}) = N\pi r^2\left(1-\frac{C_a^{IO}}{\pi r^2}\right) \quad (5)$$

6) Total Overlapped Coverage Area

The total overlapped coverage area C_a^{TO} of a deployment pattern is the total area covered by more than one sensors. In terms of precision agriculture, it defines the overall coverage interference area within the form consequently resulting in coverage capability depletion and coverage quality degradation by redundant sensors. It can be measured as expressed by Eq. (6).

$$C_a^{TO} = C_a^T - C_a^{TNO} = C_a^T - \left\{N\pi r^2\left(1-\frac{C_a^{IO}}{\pi r^2}\right)\right\} \quad (6)$$

7) Quality of Connectivity

The quality of connectivity Q_c of a deployment pattern defines the communication quality among the geometrically sensors. Apart from the impact of the geometrical pattern followed in a particular deployment, quality of communication medium or environment also significantly affects the quality of connectivity of a deployment pattern. In terms of precision agriculture, it defines the overall quality of the system employed to enhance and ease agriculture process. It can be measured as expressed by Eq. (7).

$$Q_c = \frac{K\,C_a^{TO}}{C_a^E} = \frac{K\left[C_a^T - \left\{N\pi r^2\left(1-\frac{C_a^{IO}}{\pi r^2}\right)\right\}\right]}{\frac{C_a^{TO}+C_a^{TNO}}{N\pi r^2}} = \frac{KN\pi r^2\{C_a^T - N\pi r^2 + N\,C_a^{IO}\}}{C_a^T}$$

$$= KN\pi r^2\left\{1 - \frac{N\pi r^2}{C_a^T} + \frac{N\,C_a^{IO}}{C_a^T}\right\} \quad (7)$$

where, K is the quality of connectivity conversion constant. For ideal case K = 1 has been considered. The quality of connectivity has been normalized to obtain the value of quality of connectivity in the defined range.

8) Multi-objective Optimization

The aforementioned seven metrics are considered as objective functions of the Multi-objective Optimization (MOO) formulation. The formulation can be expressed as given by Eq. (8).

$$Max(f_1, f_2, f_3, f_4, f_5, f_6^{-1}, f_7) \quad (8)$$

where $f_1 = C_a^T$ represents total coverage area, $f_2 = C_a^E$ represents effective coverage area, $f_3 = C_a^{NE}$ represents net effective coverage area, $f_4 = C_a^{NER}$ represents net effective coverage area ratio, $f_5 = C_a^{TNO}$ represents total no-overlapped coverage area, $f_6^{-1} = (C_a^{TO})^{-1}$ represents total overlapped coverage area, and $f_7 = Q_c$ represents quality of connectivity. The constraints of each metric denotes the constraints of the MOO formulation. The constraints include $C_a^T \leq NC_a^1$, $\frac{1}{N} \leq C_a^E \leq 1, 0 < C_a^{NE} \leq \pi r^2, 0 < C_a^{NER} \leq 1$.

The cost of deployment has significant impact on the overall cost of WSNs in case of heterogeneous sensors or hostile environments [36]. Thus, it could be considered as a metric. However, uniform quality of coverage requirement and ease of access of farming regions reduce the relevance of cost of deployment in precision agriculture using WSNs.

B. The Measurements

The aforementioned metrics for measuring quality of coverage and connectivity are utilized to evaluate four geometrical model based deployment patterns. The exact mathematical derivation of all the metrics are obtained for each deployment pattern exploiting their geometrical characteristics. Using the mathematical derivations, each of the metric has been quantified which can be used to compare the quality of coverage and connectivity of deployment patterns.

1) Metric Quantification in Square Pattern based forming

Square deployment pattern is one of simplest deployment approach in WSNs. Two cases of square deployment pattern are explored. In the first case, nine sensors are deployed at the vertices of four adjoining squares (see Fig. 2(a)). In the second case, sixteen sensors are deployed at the vertices of nine adjoining squares (see Fig. 2(b)). The length of side of squares is considered equal to the sensing range of sensors in both the cases of measurement.

- *Total Coverage Area*

$$C_a^T = 4(\diamond AS_1H) + 4(\diamond AS_2B) + 8(\Delta AS_1S_2) + \square S_1S_3S_9S_7$$
$$= 4\left(\frac{150}{360}\pi r^2\right) + 4\left(\frac{\pi}{6}r^2\right) + 8\left(\frac{\sqrt{3}}{4}r^2\right) + 4r^2 = \left(\frac{7\pi}{3} + 2\sqrt{3} + 4\right)r^2 \quad (9)$$

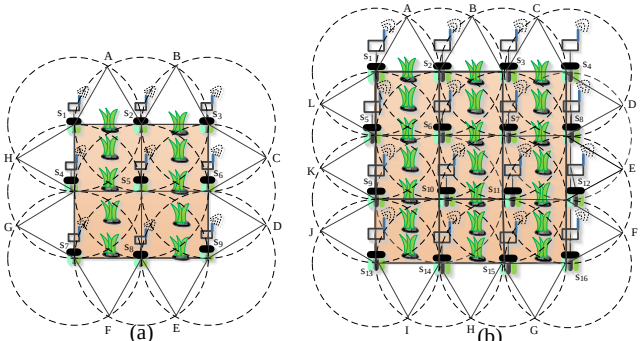

Fig. 2. Square pattern based forming (a) Nine sensors (b) sixteen sensors

- *Effective Coverage Area*

$$C_a^E = \frac{C_a^{TO}+C_a^{TNO}}{N\pi r^2} = \frac{\left(\frac{7\pi}{3}+2\sqrt{3}+4\right)r^2}{9\pi r^2} = \frac{7}{27} + \frac{2\sqrt{3}}{9\pi} + \frac{4}{9\pi} = 0.52 \quad (10)$$

- *Net Effective Coverage Area*

$$C_a^{NE} = \pi r^2 - C_a^{IO} = \pi r^2 - \left\{\frac{\pi}{4}r^2 + 2\left(\frac{\pi}{6}r^2\right) + 2\left(\frac{\pi}{6}r^2 - \frac{\sqrt{3}}{4}r^2\right)\right\}$$

$$= \pi r^2 - \left\{\frac{\pi}{4}r^2 + \frac{2\pi}{3}r^2 - \frac{\sqrt{3}}{4}r^2\right\} = \frac{\pi+6\sqrt{3}}{12}r^2 \quad (11)$$

- *Net Effective Coverage Area Ratio*

$$C_a^{NER} = 1 - \frac{C_a^{IO}}{\pi r^2} = 1 - \frac{\left\{\frac{\pi}{4}r^2 + \frac{2\pi}{3}r^2 - \frac{\sqrt{3}}{4}r^2\right\}}{\pi r^2} = 0.35 \quad (12)$$

• *Total Non-overlapped Coverage Area*

$$C_a^{TNO} = N\pi r^2\left(1-\frac{C_a^{IO}}{\pi r^2}\right) = 9\pi r^2\left(1-\frac{\left\{\frac{\pi}{4}r^2+\frac{2\pi}{3}r^2-\frac{\sqrt{3}}{4}r^2\right\}}{\pi r^2}\right)$$

$$= 3\left(\frac{\pi+6\sqrt{3}}{4}\right)r^2 \quad (13)$$

• *Total Overlapped Coverage Area*

$$C_a^{TO} = C_a^T - \left\{N\pi r^2\left(1-\frac{C_a^{IO}}{\pi r^2}\right)\right\} = \left(\frac{7\pi}{3}+2\sqrt{3}+4\right)r^2 - 3\left(\frac{\pi+6\sqrt{3}}{4}r^2\right) = \left(\frac{19\pi}{12}-\frac{5\sqrt{3}}{2}+4\right)r^2 \quad (14)$$

• *Quality of Connectivity*

$$Q_c = KN\pi r^2\left\{1-\frac{N\pi r^2}{C_a^T}+\frac{N\,C_a^{IO}}{C_a^T}\right\} = 9\pi r^2\left\{1-\frac{9\pi r^2}{\left(\frac{7\pi}{3}+2\sqrt{3}+4\right)r^2}+\frac{9\left\{\frac{\pi}{4}r^2+\frac{2\pi}{3}r^2-\frac{\sqrt{3}}{4}r^2\right\}}{\left(\frac{7\pi}{3}+2\sqrt{3}+4\right)r^2}\right\} = \frac{\left(\frac{19\pi}{12}-\frac{5\sqrt{3}}{2}+4\right)r^2}{0.52} \quad (15)$$

In the second case, sixteen sensors are deployed at the vertices of nine adjoining squares (see Fig 2(b)). All the sensors S_1 to S_{16} have equal sensing range and the length of the side of square is equal to the sensing range. The quality of the sixteen sensor square deployment pattern is measured below.

• *Total Coverage Area*

$$C_a^T = 4(\diamond AS_1L) + 8(\diamond AS_2B) + 12(\Delta AS_1S_2) + S_1S_4S_{16}S_{13}$$

$$= 4\left(\frac{150}{360}\pi r^2\right) + 8\left(\frac{\pi}{6}r^2\right) + 12\left(\frac{\sqrt{3}}{4}r^2\right) + 9r^2 = (3\pi+3\sqrt{3}+9)r^2 \quad (16)$$

• *Effective Coverage Area*

$$C_a^E = \frac{C_a^{TO}+C_a^{TNO}}{N\pi r^2} = \frac{(3\pi+3\sqrt{3}+9)r^2}{16\pi r^2} = \frac{3}{16}+\frac{3\sqrt{3}}{16\pi}+\frac{9}{16\pi} = 0.47 \quad (17)$$

• *Net Effective Coverage Area*

$$C_a^{NE} = \pi r^2 - C_a^{IO} = \pi r^2 - \left\{\frac{\pi}{4}r^2+2\left(\frac{\pi}{6}r^2\right)+2\left(\frac{\pi}{6}r^2-\frac{\sqrt{3}}{4}r^2\right)\right\}$$

$$= \pi r^2 - \left\{\frac{\pi}{4}r^2+\frac{2\pi}{3}r^2-\frac{\sqrt{3}}{4}r^2\right\} = \frac{\pi+6\sqrt{3}}{12}r^2 \quad (18)$$

• *Net Effective Coverage Area Ratio*

$$C_a^{NER} = 1-\frac{C_a^{IO}}{\pi r^2} = 1-\frac{\left\{\frac{\pi}{4}r^2+\frac{2\pi}{3}r^2-\frac{\sqrt{3}}{4}r^2\right\}}{\pi r^2} = 0.35 \quad (19)$$

• *Total Non-overlapped Coverage Area*

$$C_a^{TNO} = N\pi r^2\left(1-\frac{C_a^{IO}}{\pi r^2}\right) = 16\pi r^2\left(1-\frac{\left\{\frac{\pi}{4}r^2+\frac{2\pi}{3}r^2-\frac{\sqrt{3}}{4}r^2\right\}}{\pi r^2}\right)$$

$$= 4\left(\frac{\pi+6\sqrt{3}}{3}\right)r^2 \quad (20)$$

• *Total Overlapped Coverage Area*

$$C_a^{TO} = C_a^T - \left\{N\pi r^2\left(1-\frac{C_a^{IO}}{\pi r^2}\right)\right\} = (3\pi+3\sqrt{3}+9)r^2 - 4\left(\frac{\pi+6\sqrt{3}}{3}r^2\right) = \left(\frac{5\pi}{3}+5\sqrt{3}+9\right)r^2 \quad (21)$$

• *Quality of Connectivity*

$$Q_c = KN\pi r^2\left\{1-\frac{N\pi r^2}{C_a^T}+\frac{N\,C_a^{IO}}{C_a^T}\right\}$$

$$= 16\pi r^2\left\{1-\frac{16\pi r^2}{(3\pi+3\sqrt{3}+9)r^2}+\frac{16\left\{\frac{\pi}{4}r^2+\frac{2\pi}{3}r^2-\frac{\sqrt{3}}{4}r^2\right\}}{(3\pi+3\sqrt{3}+9)r^2}\right\} = \frac{\left(\frac{5\pi}{3}+5\sqrt{3}+9\right)r^2}{0.47} \quad (22)$$

2) *Metric Quantification in Pentagon Pattern based forming*

The pentagon deployment pattern is a modified consideration of triangular deployment patter in which five sensors are deployed at the vertices of a pentagon and one sensor at the center of pentagon (see Fig. 3). The sensing range of the sensors has been considered as r and the side of the pentagon has been considered as P. The value P = $2r\tan(36^o)$ can be calculated using simple geometrical calculations. Considering radius AS_1 as tangent to the circle having center at S_5, the radius S_5A will be perpendicular to the AS_1. In other words, the angle $< S_5A\,S_1 = 90^o$ and thus, $< AS_5S_1 =< AS_1S_5 = 45^o$. The quality of coverage and connectivity of pentagon deployment pattern are measured below.

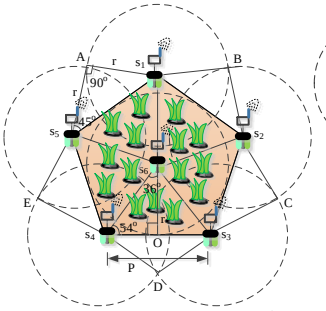

Fig. 3. Pentagon pattern based forming

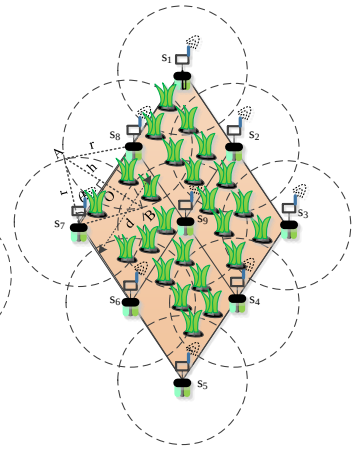

Fig. 4. Rhombus pattern based forming

• *Total Coverage Area*

$$C_a^T = 5\{\diamond AS_1B + \Delta AS_1S_5 + \Delta S_3S_4S_6\}$$

$$= 5\left\{\left(\frac{162\pi}{360}r^2\right)+\left(\frac{r^2}{2}\right)+r^2\tan(36^o)\right\} = \left(\frac{9\pi}{4}+6.13\right)r^2 \quad (23)$$

• *Effective Coverage Area*

$$C_a^E = \frac{C_a^{TO}+C_a^{TNO}}{N\pi r^2} = \frac{\left(\frac{9\pi}{4}+6.13\right)r^2}{6\pi r^2} = 0.88 \quad (24)$$

• *Net Effective Coverage Area*

$$C_a^{NE} = \pi r^2 - C_a^{IO} = \pi r^2 - \left\{\frac{108\mu}{360}r^2+2\left(\frac{45\pi}{360}r^2\right)\right\}$$

$$= \pi r^2 - \left\{\frac{11\pi}{20}r^2\right\} = \frac{9\pi}{20}r^2 \quad (25)$$

• *Net Effective Coverage Area Ratio*

$$C_a^{NER} = 1-\frac{C_a^{IO}}{\pi r^2} = 1-\frac{\left\{\frac{11\pi}{20}r^2\right\}}{\pi r^2} = 0.80 \quad (26)$$

• *Total Non-overlapped Coverage Area*

$$C_a^{TNO} = N\pi r^2\left(1-\frac{C_a^{IO}}{\pi r^2}\right) = 6\pi r^2\left(1-\frac{\left\{\frac{11\pi}{20}r^2\right\}}{\pi r^2}\right) = \frac{27}{10}r^2 \quad (27)$$

• *Total Overlapped Coverage Area*

$$C_a^{TO} = C_a^T - \left\{N\pi r^2\left(1-\frac{C_a^{IO}}{\pi r^2}\right)\right\} = \left(\frac{9\pi}{4}+6.13\right)r^2 - \frac{27}{10}r^2$$

$$= \left(\frac{9\pi}{4}+3.43\right)r^2 \quad (28)$$

• *Quality of Connectivity*

$$Q_c = KN\pi r^2\left\{1-\frac{N\pi r^2}{C_a^T}+\frac{N\,C_a^{IO}}{C_a^T}\right\} = 6\pi r^2\left\{1-\frac{6\pi r^2}{C_a^T}+\frac{6\left\{\frac{11\pi}{20}r^2\right\}}{C_a^T}\right\} = \frac{\left(\frac{9\pi}{4}+3.43\right)r^2}{0.88} \quad (29)$$

3) *Metric Quantification in Rhombus Pattern based forming*

In rhombus deployment pattern, sensors are deployed at the vertices of adjoining rhombus. Following the pattern, nine sensors are deployed at the vertices of rhombus (see Fig. 4). In this deployment pattern, the intersection coverage area between any two sensors is always equal. To determine the intersection coverage area, the distance between the sensors is considered as d. The angle $\theta = \cos^{-1}(d/2r)$ is derived using

trigonometry rules. The value $h = \sqrt{r^2 - (d/2)^2}$ is derived using triangle rules and it is used to calculate the area of $\Delta AS_7B = d\left(\sqrt{r^2 - (d/2)^2}\right)/2$. The intersection coverage area between the two sensors s_7 and s_8 can be derived subtracting the area of the triangle ΔAS_7B from the area of the sector $AS_7B = \theta r^2$. Thus, the intersection coverage area is $2\left\{\theta r^2 - \left(d\left(\sqrt{r^2 - (d/2)^2}\right)/2\right)\right\}$ .The quality of coverage and connectivity of rhombus deployment pattern is measured through following derivations.

- *Total Coverage Area*

$$C_a^T = 9(\pi r^2) - 16\left(2\left\{\theta r^2 - \left(d\left(\sqrt{r^2 - (d/2)^2}\right)/2\right)\right\}\right)$$

To simplify the calculation, d = r is considered. In other words, the sensing range of two neoghboring sensors passes through the centers. Thus, the value of $\theta = 60^o$ can be derived using simple geometrical calculations. The the value of C_a^T can be calculated as expressed by Eq. (30).

$$C_a^T = 9(\pi r^2) - 16\left\{\frac{(2\pi - 3\sqrt{3})r^2}{6}\right\} = \left(\frac{11\pi}{3} + 8\sqrt{3}\right)r^2 \quad (30)$$

- *Effective Coverage Area*

$$C_a^E = \frac{C_a^{TO} + C_a^{TNO}}{N\pi r^2} = \frac{\left(\frac{11\pi}{3} + 8\sqrt{3}\right)r^2}{9\pi r^2} = 0.7 \quad (31)$$

- *Net Effective Coverage Area*

$$C_a^{NE} = \pi r^2 - C_a^{IO} = \pi r^2 - 2\left\{\frac{(2\pi - 3\sqrt{3})r^2}{6}\right\} = \left(\frac{\pi + 3\sqrt{3}}{3}\right)r^2 \quad (32)$$

- *Net Effective Coverage Area Ratio*

$$C_a^{NER} = 1 - \frac{C_a^{IO}}{\pi r^2} = 1 - \frac{2\left\{\frac{(2\pi - 3\sqrt{3})r^2}{6}\right\}}{\pi r^2} = 0.45 \quad (33)$$

- *Total Non-overlapped Coverage Area*

$$C_a^{TNO} = N\pi r^2\left(1 - \frac{C_a^{IO}}{\pi r^2}\right) = 9\pi r^2\left(1 - \frac{2\left\{\frac{(2\pi - 3\sqrt{3})r^2}{6}\right\}}{\pi r^2}\right) = 3(\pi + 3\sqrt{3})r^2 \quad (34)$$

- *Total Overlapped Coverage Area*

$$C_a^{TO} = C_a^T - \left\{N\pi r^2\left(1 - \frac{C_a^{IO}}{\pi r^2}\right)\right\} = \left(\frac{11\pi}{3} + 8\sqrt{3}\right)r^2 - 3(\pi + 3\sqrt{3})r^2 = \left(\frac{2\pi}{3} - \sqrt{3}\right)r^2 \quad (35)$$

- *Quality of Connectivity*

$$Q_c = KN\pi r^2\left\{1 - \frac{N\pi r^2}{C_a^T} + \frac{N\,C_a^{IO}}{C_a^T}\right\} = 9\pi r^2\left\{1 - \frac{9\pi r^2}{\left(\frac{11\pi}{3} + 8\sqrt{3}\right)r^2} + \frac{92\left\{\frac{(2\pi - 3\sqrt{3})r^2}{6}\right\}}{\left(\frac{11\pi}{3} + 8\sqrt{3}\right)r^2}\right\} = \frac{\left(\frac{2\pi}{3} - \sqrt{3}\right)r^2}{0.7} \quad (36)$$

4) *Metric Quantification in Hexagon Pattern based forming*

In hexagon deployment pattern, six sensors are deployed at the vertices of hexagon and one sensor is deployed at the center of the hexagon (see Fig.5). In this deployment pattern also, the intersection coverage area between the sensing range of any two sensors is always equal. The calculation of intersection coverage area in hexagon deployment is similar to what is performed to calculate intersection area in rhombus deployment pattern. Following the steps, the intersection coverage area in hexagon deployment can be calculated as $2\left\{\theta r^2 - \left(d\left(\sqrt{r^2 - (d/2)^2}\right)/2\right)\right\}$. The quality of coverage and connectivity of hexagon deployment pattern is measured below.

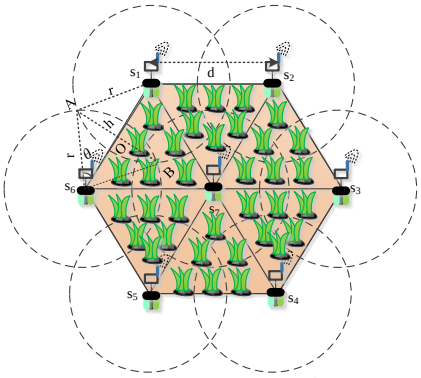

Fig. 5. Hexagon pattern based forming

- *Total Coverage Area*

$$C_a^T = 7(\pi r^2) - 12\left(2\left\{\theta r^2 - \left(d\left(\sqrt{r^2 - (d/2)^2}\right)/2\right)\right\}\right)$$

Here in this section also, the case has been simplified with same assumption as considered in case of rhombus deployment; i.e., d = r. With this assumption, total coverage area C_a^T can be calculated as expressed by Eq. (37).

$$C_a^T = 7(\pi r^2) - 12\left\{\frac{(2\pi - 3\sqrt{3})r^2}{6}\right\} = (3\pi + 6\sqrt{3})r^2 \quad (37)$$

- *Effective Coverage Area*

$$C_a^E = \frac{C_a^{TO} + C_a^{TNO}}{N\pi r^2} = \frac{(3\pi + 6\sqrt{3})r^2}{7\pi r^2} = \frac{3}{7} + \frac{6\sqrt{3}}{7\pi} = 0.90 \quad (38)$$

- *Net Effective Coverage Area*

$$C_a^{NE} = \pi r^2 - C_a^{IO} = \pi r^2 - 3\left\{\frac{(2\pi - 3\sqrt{3})r^2}{6}\right\} = \frac{3\sqrt{3}}{2}r^2 \quad (39)$$

- *Net Effective Coverage Area Ratio*

$$C_a^{NER} = 1 - \frac{C_a^{IO}}{\pi r^2} = 1 - \frac{3\left\{\frac{(2\pi - 3\sqrt{3})r^2}{6}\right\}}{\pi r^2} = \frac{\frac{3\sqrt{3}}{2}r^2}{\pi r^2} = 0.82 \quad (40)$$

- *Total Non-overlapped Coverage Area*

$$C_a^{TNO} = N\pi r^2\left(1 - \frac{C_a^{IO}}{\pi r^2}\right) = 7\pi r^2\left(1 - \frac{3\left\{\frac{(2\pi - 3\sqrt{3})r^2}{6}\right\}}{\pi r^2}\right) = \left(\frac{21\sqrt{3}}{2}\right)r^2 \quad (41)$$

- *Total Overlapped Coverage Area*

$$C_a^{TO} = C_a^T - \left\{N\pi r^2\left(1 - \frac{C_a^{IO}}{\pi r^2}\right)\right\} = (3\pi + 6\sqrt{3})r^2 - \left(\frac{21\sqrt{3}}{2}\right)r^2 = \left(3\pi - \frac{9\sqrt{3}}{2}\right)r^2 \quad (42)$$

- *Quality of Connectivity*

$$Q_c = KN\pi r^2\left\{1 - \frac{N\pi r^2}{C_a^T} + \frac{N\,C_a^{IO}}{C_a^T}\right\} = 7\pi r^2\left\{1 - \frac{7\pi r^2}{(3\pi + 6\sqrt{3})r^2} + \frac{21\left\{\frac{(2\pi - 3\sqrt{3})r^2}{6}\right\}}{(3\pi + 6\sqrt{3})r^2}\right\} = \frac{\left(3\pi - \frac{9\sqrt{3}}{2}\right)r^2}{0.90} \quad (43)$$

IV. Empirical Results

In this section, analytical, simulation and testbed results are discussed for measuring the quality of coverage and connectivity of deployment patterns in terms of the considered metrics. This section is broadly divided into three parts. In the first part, the analytical results are discussed whereas in the second and third parts simulation and testbed results are discussed; respectively.

A. Analytical Results

In this section, the derivations obtained in terms of coverage and connectivity metrics for each of the considered deployment pattern are analytically evaluated using mathematical tool. The sensing range $r = 15$ m and transmission range $t = 25$ m are considered while measuring coverage to focus on coverage metrics whereas both sensing range and transmission range are considered equal; i.e., $r = t = 15$ m for measuring connectivity to focus on connectivity metric.

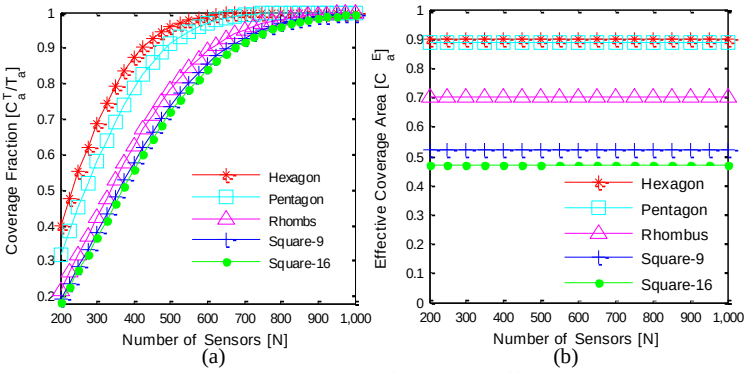

Fig. 6. Analytical results: (a) coverage fraction, (b) effective coverage area

Fig.6 (a) shows the impact of sensor density on coverage fraction of deployment patterns. The coverage fraction is defined as ratio of total covered sensing area and total area of sensing field considered for the experiment. It can be clearly observed that hexagon deployment pattern provides 100% coverage with least number of sensors; i.e., approximately with 620 sensors. All the other considered deployment patterns require more number of sensors for providing 100% coverage as compared to hexagon deployment. Specifically, the number of sensors required for providing 100% coverage is approximately 720 for pentagon and it is above 900 for all the other considered deployment patterns. Therefore, hexagonal deployment pattern is far better than other deployment patterns in providing coverage fraction. The results in Fig.6 (b) show the impact of sensor density on effective coverage area C_a^E of deployment pattern. The results reveal that sensor density has negligible impact on effective coverage area of the considered deployment patterns. The results confirm the constant values of effective coverage area obtained in the derivations in previous section for each of the considered deployment pattern. In particular, the effective coverage area for hexagonal and pentagon deployment patterns are approximately equal to 0.9 whereas it is 0.7 for rhombus and near 0.5 for both the considered square deployment patterns.

Fig. 7(a) shows the impact of sensor density on net effective coverage area C_a^{NE} of deployment patters. It can be clearly observed from the results that hexagon deployment pattern offers higher net effective coverage area as compared to those of the other considered deployment patterns. This can be attributed to the fact that the overlapping of coverage area is lower in hexagon as compared to the other deployment patterns. Pentagon deployment pattern offers lesser net effective coverage area as compared to hexagon deployment but the net effective coverage area offered by pentagon deployment is closer to what is offered by hexagon deployment for each of the considered density of sensors. The net effective coverage area offered by the other deployment patterns which includes rhombus, square-9 and square-16 are far less than what is offered by hexagon or pentagon deployment patterns due to the higher coverage overlapping.

The results in Fig. 7(b) show the impact of sensor density on net effective coverage area ratio C_a^{NER} of the deployment patterns. The results reveal that sensor density has negligible impact on net effective coverage area ration of the considered deployment patterns. The results attest the constant values obtained for net effective coverage area ratio metric in the derivations of the metric in previous section for each of the considered deployment patterns. In particular, the net effective coverage area ratio of hexagon deployment pattern is noted as 0.82 which is the maximum value of net effective coverage area among the considered deployment patterns. The value of C_a^{NER} of pentagon deployment pattern is 0.8 which is close to the value offered by hexagon. The value of C_a^{NER} for the other considered deployment patterns is far below than 0.5. Two different deployment strategies considered under square deployment pattern show equal value of net effective coverage area ratio due to the similar geometrical shape resulting in equal coverage overlapping within an individual sensor's coverage area.

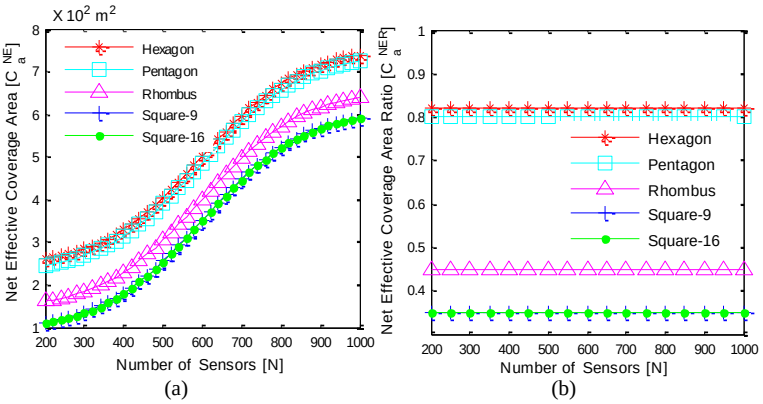

Fig.7. Analytical results: (a) net effective coverage area, (b) net effective coverage area ratio

Fig.8 (a) demonstrate the impact of sensor density on total overlapped coverage area C_a^{TO} of the deployment patterns. The rapid increment in total overlapped coverage area for all the deployment patterns can be clearly observed from the results. The total overlapped coverage area in hexagon deployment pattern is smaller than that of other deployment patterns for each of the sensor density taken into consideration. In case of pentagon, C_a^{TO} is definitely bigger than that of hexagon but it is closer to the hexagon's C_a^{TO} as compared to the rhombus and square deployment patterns. . This is because of geometrical shape similarity between pentagon and hexagon. The results in Fig.8 (b) show the impact of sensor density on quality of connectivity of the network. Square deployment patterns offer higher quality of connectivity among the considered deployment patterns which confirms the derivation of quality of connectivity carried out in previous section. For all the deployment patterns considered, quality of connectivity of the network is approximately constant up to 500 sensors and it increases linearly when number of sensors are more than 500. This can be attributed to the fact that till

500sensors coverage overlapping is lesser as evident from Fig. 8(a). Once the closeness of sensors increase with more than 500 sensors, the better quality of connectivity is noted for the deployment patterns.

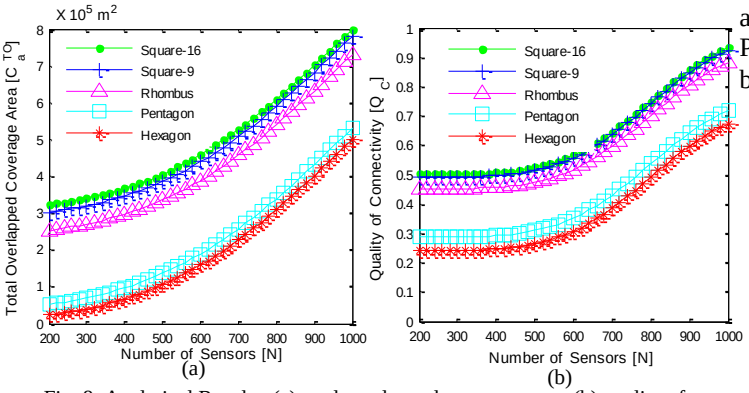

Fig. 8. Analytical Results: (a) total overlapped coverage area, (b) quality of connectivity

1) Analysis of the Multi-objective Optimization

In MOO, a better solution or Pareto optimal solution $S(*)$ in comparison with another solution $S(A)$ is defined as $\forall\, i \in \{1,2,\dots,7\}, S(*)_i \preccurlyeq S(A)_i \wedge \exists\, i \in \{1,2,\dots,7\}, S(*)_i > S(A)_i$. The set of all Pareto solutions in the objective space is mapped to Pareto optimal Front (PF) [37]. Due to the number of metrics considered, a solution which optimizes all the metrics with maximum values at the same time, rarely exists. Therefore, Pareto optimal solutions are aimed. This analysis would provide some insights of the properties and features of the solutions in the PF of the MOO. Three different set of objectives are considered for analysis due to the number of direction representation in space. In Fig. 9(a), the objectives including $f_1 = C_a^T, f_2 = C_a^E$ and $f_3 = C_a^{NE}$ are considered. The optimal solution is designed analytically considering each objective. The optimal solution considering objective f_1 is represented by $S(C_a^T)$ which has maximum C_a^T but minimum C_a^E and C_a^{NE}. The maximum value of C_a^T and minimum value of C_a^E and C_a^{NE} represented by the solution $S(C_a^T)$, i.e., $C_a^T\left(S(C_a^T)\right) = \max(C_a^T), C_a^E\left(S(C_a^T)\right) = min(C_a^E)$ and $C_a^{NE}\left(S(C_a^T)\right) = min(C_a^{NE})$ can be defined and normalized with the help of the constraints of the corresponding metrics. The optimal solution considering objective f_2 is represented by $S(C_a^E)$ which has maximum C_a^E but minimum C_a^T and C_a^{NE}. The optimal values of the metrics defined by the solution $S(C_a^E)$, i.e., $C_a^E\left(S(C_a^E)\right) = \max(C_a^T), C_a^T\left(S(C_a^E)\right) = min(C_a^T)$ and $C_a^{NE}\left(S(C_a^E)\right) = min(C_a^{NE})$ can be generated and normalized considering the related constraints. The optimal solution considering objective f_3 is represented by $S(C_a^{NE})$ which has maximum C_a^{NE} but minimum C_a^T and C_a^E. The maximum value of C_a^{NE} and minimum value C_a^T and C_a^E, i.e., $C_a^{NE}\left(S(C_a^{NE})\right) = max(C_a^{NE}), C_a^T\left(S(C_a^{NE})\right) = min(C_a^T)$ and $C_a^E\left(S(C_a^{NE})\right) = min(C_a^E)$ can be obtained and normalized based on the corresponding constraints of the metrics. However, the Pareto optimal solutions $PF - \{S(C_a^T), S(C_a^E), S(C_a^{NE})\}$ are more significant, because some of these solutions optimize all the three objectives at the same time. These solutions are represented by $S(C_a^T, C_a^E, C_a^{NE})$. Similar observations can be made in Fig. 9(b) where the other three objectives including $f_4 = C_a^{NER}, f_5 = C_a^{TNO}$ and $f_6^{-1} = (C_a^{TO})^{-1}$ are considered. The optimal solutions considering objectives f_4, f_5 and f_6^{-1} are represented by $S(C_a^{NER}), S(C_a^{TNO})$ and $S((C_a^{TO})^{-1})$, respectively. However, the more significant Pareto optimal solution is represented by $S(C_a^{NER}, C_a^{TNO}, (C_a^{TO})^{-1})$.

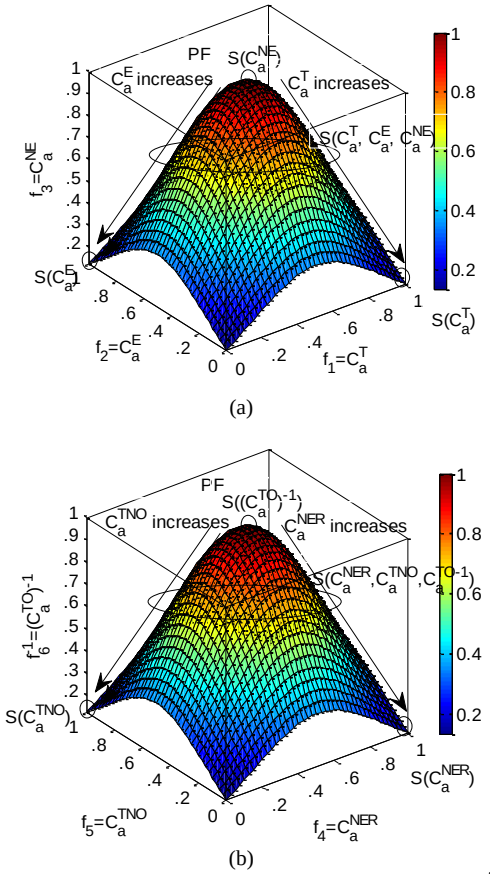

Fig. 9. The solution characteristics of the MOO: (a) with $\boldsymbol{f_1 = C_a^T, f_2 = C_a^E}$ and $\boldsymbol{f_3 = C_a^{NE}}$, (b) with $\boldsymbol{f_4 = C_a^{NER}, f_5 = C_a^{TNO}}$ and $\boldsymbol{f_6^{-1} = \left(C_a^{TO}\right)^{-1}}$

B. Simulation Results

In this section, simulations are performed in Network Simulator (NS-2) to measure the performance of deployment patterns in terms of quality of coverage and connectivity in realistic environment for verifying the analytical results obtained in the previous section. The simulation experiments are conducted for each of the deployment patterns considered one-by-one. For each experiments, simulation area of $1500 \times 1500\ \mathrm{m}^2$ is considered and sensors are deployed in the range $200 - 1000$ following a particular deployment patterns. After following a particular pattern, the impact of exceeded sensors is not considered for simplicity in comparative evaluation. For example, with 200 sensors in the network, 2 sensors exceeded in square-9, rhombus and pentagon, 4 sensors exceeded in hexagon, and 8 sensors exceeded in square-16 deployment patterns. Two percent sensors are randomly selected as active senders for communication in each experiment. Each sensor generates data following Poisson process of rate μ, where $1/\mu = 0.1/s$. In each experiment, the destination sensor is changed following

exponential distribution of rate $\delta = {}^{1}/_{20}\,ms$. During the simulation of coverage metric, sensing range r = 15 m and transmission range t = 25 m are considered for focusing on coverage measurement. For quality of connectivity measurement, both sensing range and transmission range are considered equal; i.e., r = t = 15 m. The data rate considered in the simulation for communication among sensor nodes is 40 kbps. Propagation delay during transmission has been considered negligible taking into account the specified simulation area. The basic parameter values used in the simulations are summarized in Table-2. Each experiment has been repeated 30 times over different seeds and average has been taken for data record utilized in the results with 95% confidence interval.

Table 2. Basic parameter setting for simulations

Parameter	Value	Parameter	Value
Simulation area	$1500 \times 1500\ m^2$	Packet Type	UDP
Simulation time	$600s$	Ifqlen	50
No of sensors	$200 - 1000$	Channel Type	$Wireless$
Bandwidth	40 Kbps	Propagation model	$Shadowing$
t	$15m\ and\ 25\ m$	Antenna Model	$Omni\ dir.$
r	$15m$	MAC protocol	$IEEE$ 802.11
Data senders	$2\%\ sensors$	Query period	$3s$
$1/\mu$	$0.1/s$	Hello timeout	$1s$
δ	$1/20\ ms$	Packet Type	UDP

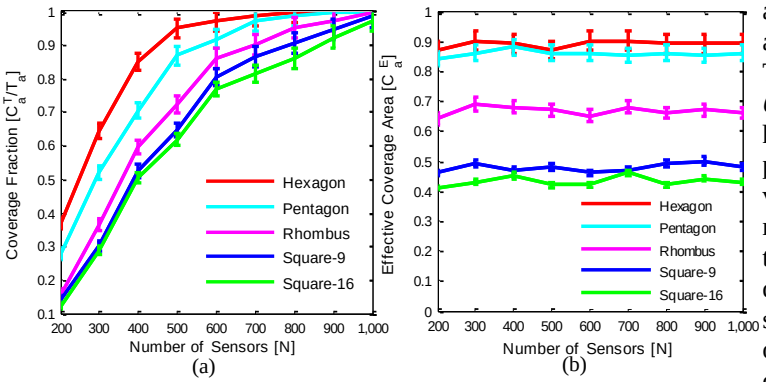

Fig. 10. Simulation Results: (a) coverage fraction, (b) effective coverage area

Simulation results shown in Fig. 10(a) corroborate the analytical results of coverage fraction. It can be clearly observed that hexagon deployment pattern provides higher coverage fraction with lesser number of sensors as compared to the other regular deployment patterns considered. Although the coverage fractions obtained through simulations is lesser from the estimated coverage fraction in analytical results for each of sensor density considered but they are very close the analytically estimated coverage fractions. For example, N = 500 sensors, the coverage fraction offered by hexagon deployment is 0.93 in simulation whereas it is 0.98 in analytical results as depicted in Fig. 6(a). Simulation results shown in Fig. 10(b) confirm the corresponding analytical results for effective coverage area. In simulation results, effective coverage area provided by the considered deployment patterns are not exactly constant as estimated in analytical results but they are slightly varying around constant values observed in analytical results. Hexagon deployment pattern which provide bigger effective coverage area among the considered deployment patterns in analytical results is validated by simulation results. For example, for N = 600 − 1000 sensors, the constant value of effective coverage area for hexagon deployment pattern is approximately 0.89 which is close to what is noted in analytical results; i.e., 0.9.

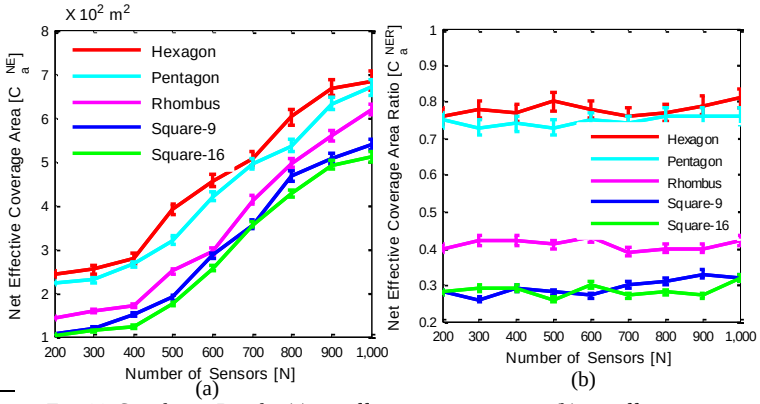

Fig. 11. Simulation Results (a) net effective coverage area, (b) net effective coverage area ratio

Simulation results depicted in Fig. 11(a) verifies the analytical results for net effective coverage area metric. The increment in C_a^{NE} with the increase in number of sensors is similar to what is observed in analytical results. For example, N = 200, 600 and 1000, hexagon deployment offers approximately 230, 440 and 690 m^2 net effective coverage area; respectively, whereas it offers approximately 260, 480 and 706 m^2 net effective coverage area in analytical results. The other deployment patterns also offer similar increment in C_a^{NE} to what is offered in analytical results. Therefore, the higher net effective coverage area offered by hexagon and pentagon deployments due to lower coverage overlapping is verified by simulation results. Fig. 11(b) shows simulation results for net effective coverage area ratio metric and attest the observed constant values in analytical results for each deployment pattern. Although C_a^{NER} is not exactly constant in simulation results yet, it is varying near the constant values observed in analytical results. Specifically, net effective coverage area ratio of hexagon deployment varies in the range 0.78 − 0.81 in simulation results which close to the constant value of 0.81 observed in analytical results. Similarly, the ratio of pentagon deployment varies in the range 0.75 − 0.78 in simulation results which is also close to the constant value of 0.8 observed in analytical results. It is also noteworthy that there is slight fluctuation in the net effective coverage area ratio of square-9 and square-16 deployment patterns due to the difference of number of exceeded sensors after following these two deployment patterns in the network with specified number of sensors. Thus, the higher and constant net effective coverage area ratio provided by both hexagon and pentagon deployments in analytical results are attested by simulation results.

Total overlapped coverage area of deployment patterns measured through simulation is shown in Fig.12 (a). Simulation results attest the lower coverage overlapping provided by hexagon and pentagon deployment patters in analytical results. The results also verify the higher coverage overlapping of square deployment patterns. For example, $N = 200$, the total overlapped coverage area of hexagon and pentagon deployments are 1275 and 2575 m^2; respectively, which are lower as compared to that of other deployment

patters. For $N = 1000$, the total overlapped coverage area of square-16 and square-9 deployments are 71000 and 66000 m^2; respectively, which are higher as compared to that of other deployment patters. Simulation results of quality of connectivity of deployment patterns is shown in Fig. 12(b) which contradict with what is observed in analytical results due to the no consideration of interference in the derivation of the metric. Specifically, quality of connectivity of hexagon deployment pattern is higher due to the lower coverage overlapping resulting in lower interference. Quality of connectivity is lower for square deployment patterns due to the higher interference resulting from higher coverage overlapping. Therefore, in realistic simulation scenario, the quality of connectivity is considerably affected by interference of the network resulting from coverage overlapping.

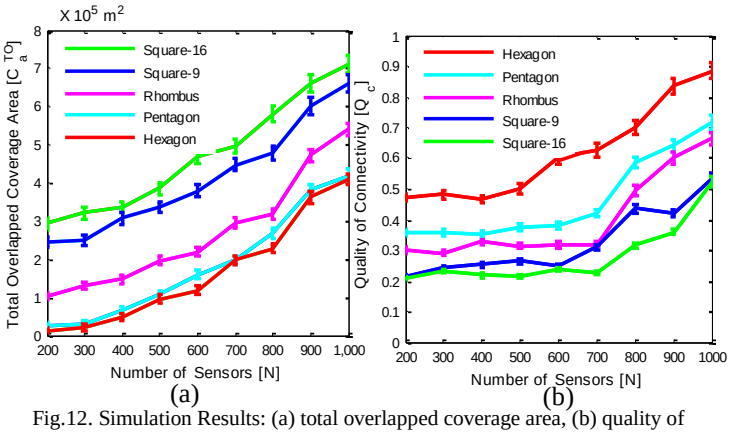

Fig.12. Simulation Results: (a) total overlapped coverage area, (b) quality of connectivity

C. *Testbed Results*

In this section, sensor deployment patters are evaluated in 'INDRIYA' wireless sensor network testbed of the School of Computing, National University of Singapore (NUS) [22]. Total 139 number of wireless sensor network nodes which are commonly known as motes N_m are available in the testbed for experiment. Most of the motes are in good condition and available to researchers for experiment through online and offline ways. There are four types of sensors utilized in these motes; namely, WiEye, SBT30, SBT80 and TelosB. The different kinds of motes are used for monitoring different activities required for precision agriculture use case.

As an example experiment, the deployment of motes is depicted in Fig. 13 where different deployment patterns are implemented in different sets of motes of 'INDRIYA'. Different set of motes are selected for implementing the considered deployment patterns. The set of nodes are selected in such a way that the patterns can be implemented with minimum possible error in terms of geometrical model. Some of the example of patterns are as follows. For square deployment pattern the set of motes that can be selected from the 1st set are 13, 11, 21, 8, 12, 19, 1, 16 and 22. Pentagon and rhombus deployment patterns can be implemented in 2nd set using the motes 70, 72, 77, 71, 84, 76 and 52, 74, 67, 75, 69, 62, 68, 60, 63; respectively. Hexagonal deployment patterns can be implemented in 3rd set with the motes 90, 103, 124, 137, 139, 104 and 97. The probability of connectivity of most of links among the motes is 1.0 and very few links are connected with probability in between 0.8 and 1.0, 0.6 and 0.8, and less than 0.6. The connectivity is measured at the default maximum transmission power $0dBM$. Some physical characteristics of the devices used in the motes are shown in Table-3. For measuring coverage area, monitoring of activities related to precision agriculture is carried out and the measured sensory data of the motes are analyzed. Thirty measurements are performed for each different types of deployment patterns. Flowchart of the workflow of the testbed implementation is provided in Fig. 14.

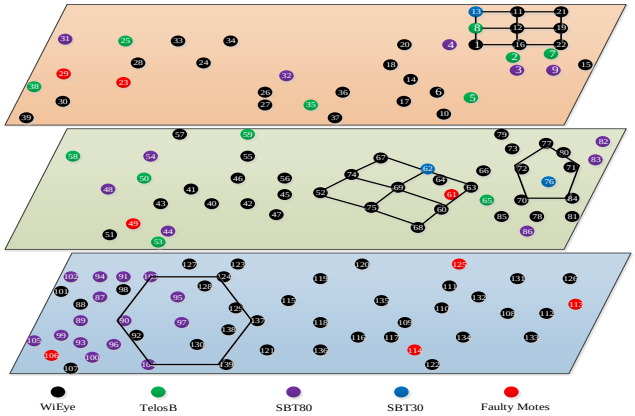

Fig. 13. Implementation of the patterns using the motes of 'INDRIYA'

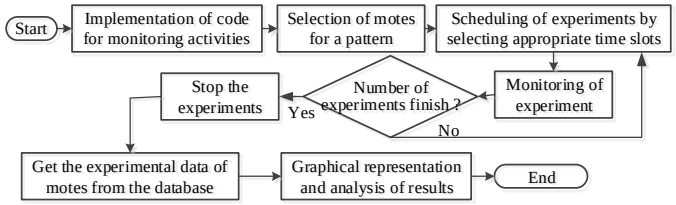

Fig.14. Workflow diagram for Testbed experiment

Table 3. Physical characteristics of the motes

Characteristics	Value	Characteristics	Value
Processor	16 bit and 8 MHz	Internal Flash	48 KB
ADC	12 bit	Sensitivity	-95dBm
RAM	10 KB	Transceiver	250 Kbps
RF chip	TI-2420	Microcontroller	TI-MSP430

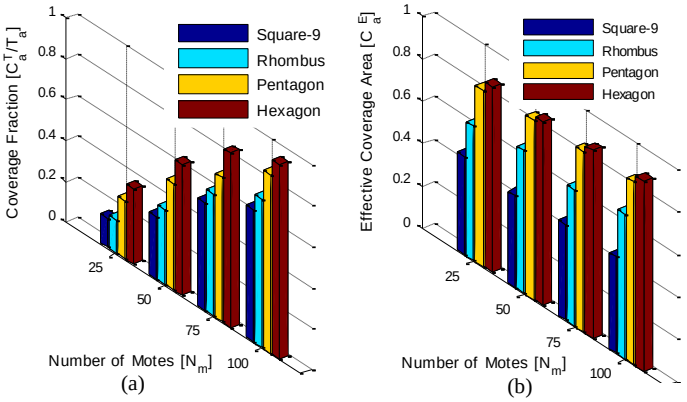

Fig.15. Testbed Results; (a) coverage fraction, (b) effective coverage area

Testbed results shown in Fig. 15(a) validates the simulation and analytical results for coverage fraction metric of deployment patterns. It can be clearly observed that the coverage fraction obtained of hexagon and pentagon deployment patterns are higher as compared to the rhombus and square deployment patterns. This is because of the

geometrical shape property of hexagon which results in lower coverage overlapping. The lower coverage overlapping significantly enhances coverage fraction of hexagon and pentagon deployment patterns. The higher effective coverage area in hexagonal deployment pattern is noted in testbed results shown in Fig. 15 (b) which attest the simulation and analytical results of effective coverage area metric. The impact of number of motes on effective coverage area is negligible and the values are constants. Specifically, net effective coverage area noted for hexagon and pentagon deployment patterns are above 0.8 which is quite similar to what is observed in simulation and analytical results. The effective coverage area observed for rhombus and square deployment are above 0.4 and 0.6; respectively, which are also similar to the noted values in simulation and analytical results.

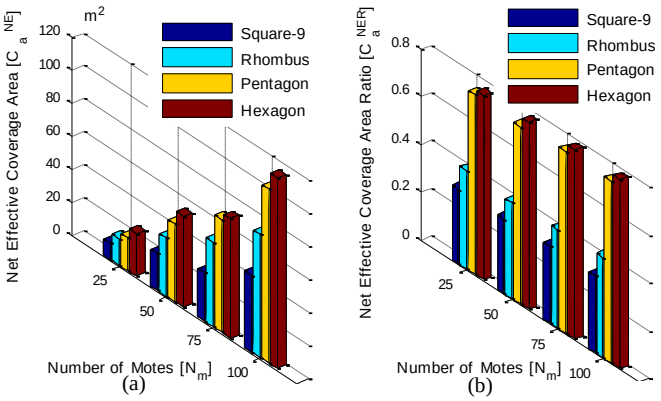

Fig.16. Testbed Results; (a) net effective coverage area, (b) net effective coverage area ratio

Testbed results shown in Fig. 16(a) validates the simulation and analytical results for net effective coverage area metric of deployment patterns. The continuous increment of net effective coverage area with the increase in number of motes is clearly the same observation what it is noted in simulation and analytical results. The size of net effective coverage area noted in testbed results is smaller than what it is observed in simulation and analytical results due to the lesser number of motes available for experiment in the testbed. Specifically, the maximum net effective coverage area noted in testbed results is less than $120\,m^2$ whereas it is $700\,m^2$ in simulation and testbed results. The constant values of net effective coverage area ratio metrics of deployment patterns observed in testbed results are depicted in Fig 16(b) which strongly validate the constant values observed in analytical and simulation results for the metric. The values of the metric for hexagon and pentagon deployment patters are higher as compared to those of other deployment patters. The constant values for hexagon and pentagon deployment patterns are also close to each other. The higher and closer constant values of the metric for hexagon and pentagon deployment is similar to what is observed in simulation and analytical results.

Testbed results in Fig. 17(a) attest the higher coverage overlapping in square deployment pattern as compared to the hexagon and pentagon deployment patterns which is observed in simulation and analytical results as well. Although the size of the total overlapped coverage area noted in testbed results is smaller than what it is observed in simulation and analytical results yet, the increment pattern with the increase of number of motes is quite similar to the simulation and analytical results. The difference in total overlapped coverage area is due to the lesser number of motes available for experiment in testbed as compared the number of sensors considered in simulation and analytical results. The better quality of connectivity in hexagon deployment pattern is observed in testbed results depicted in Fig. 17 (b) which confirms the simulation and analytical results regarding quality of connectivity. This can be attributed to the fact that the lower total overlapped coverage area is noted in hexagonal deployment pattern resulting in lower interference and better quality of connectivity as compared to the other deployment patterns. Due to the deployment of motes in precisely calculated locations at the three floors of NUS, the quality of connectivity is stable in testbed results which can be noticed as constant values for deployment patterns.

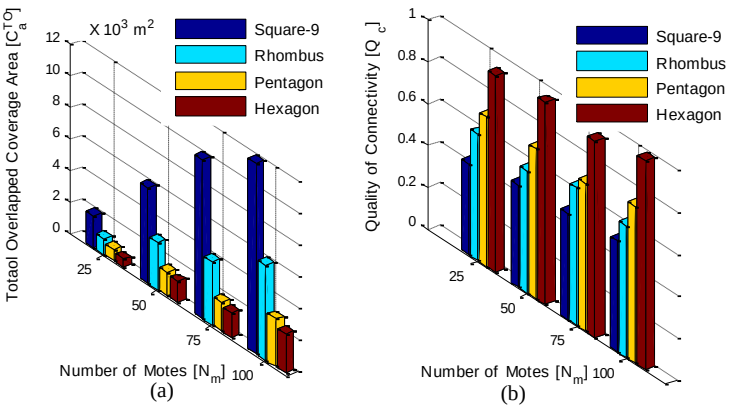

Fig.17. Testbed Results; (a) total overlapped coverage area, (b) quality of connectivity

D. Summary of Observations

From the derivation, implementation and analysis of experimental results, following is the summary of observations. The metrics for measurement of quality of coverage and connectivity are closely inter-related and have considerable impact on each other. The coverage overlapping resulting in interference substantially impacts the quality of connectivity of deployment patterns. Due to the geometrical shape property, lower coverage overlapping is observed in case of hexagon deployment pattern. The performance of hexagon and pentagon deployment is better as compared to rhombus and square deployment in case of most of the considered metrics. The larger total overlapped coverage area is observed for square deployment patterns. Analytical results shows the performance of deployment patterns in ideal environment whereas simulation results shows the performance of deployment patterns in realistically modelled environment. The testbed results shows the performance of deployment patterns in real environment.

V. Conclusion and Future Work

In this paper, a Testbed based Multi-metric Quality Measurement (T-MQM) of sensor deployment patterns for precision agriculture using WSNs is presented. The seven metrics are derived and quantified for four sensor deployment patterns in precision agriculture to measure the quality of coverage and connectivity. The measurement practically

evaluates the quality of coverage and connectivity of deployment patterns in precision agriculture through testbed implementation. The measurements and evaluations through analytical and simulation based studies which are validated using testbed experiments, are accurate and helpful for realistic implementations. The measurement should be useful for practitioners in developing performance guaranteed applications for precision agriculture whereas it should be useful for researchers in developing novel coverage and connectivity models for deployment patterns. In future research work, authors will explore three dimensional deployment patterns for precision agriculture. The impact of external interferers on quality of coverage and connectivity and development of hybrid deployment pattern exploiting mathematical geometry will also be the quest.

REFERENCES

[1] L.M. Borges, F.J. Velez, and A.S. Lebres, "Survey on the characterization and classification of wireless sensor network applications," IEEE Commun. Surveys & Tutorials, vol. 16, no. 4, pp.1860-1890, 2014.

[2] Y. Cao, N. Wang, Z. Sun, and H. Cruickshank, "A reliable and efficient encounter-based routing framework for delay/disruption tolerant networks," IEEE Sensors Journal, vol. 15, no. 7, pp.4004-4018, 2015.

[3] O. Kaiwartya, A.H. Abdullah, Y. Cao, A. Altameem, M. Prasad, C.T. Lin and X. Liu, "Internet of Vehicles: Motivation, Layered Architecture, Network Model, Challenges and Future Aspects," IEEE Access, vol. PP, no.99,pp.1-1, 2016. doi: 10.1109/ACCESS.2016.2603219

[4] S. Halder and S. DasBit, "Design of a Probability Density Function Targeting Energy-Efficient Node Deployment in Wireless Sensor Networks," IEEE Transaction on Network and Service Management, vol. 11, no. 2, pp. 204-219, 2014.

[5] D.S. Deif and Y. Gadallah, "Classification of wireless sensor networks deployment techniques," IEEE Communications Surveys & Tutorials, IEEE, vol. 16, no. 2, pp.834-855, 2014.

[6] A.J. Phillips, N.K. Newlands, S. Liang, and B.H. Ellert, "Integrated sensing of soil moisture at the field-scale: Measuring, modeling and sharing for improved agricultural decision support," Computers and Electronics in Agriculture, vol. 107, no. 1, pp.73-88, 2014.

[7] M. Srbinovska, C. Gavrovski, V. Dimcev, A. Krkoleva, A. and V. Borozan, "Environmental parameters monitoring in precision agriculture using wireless sensor networks," Journal of Cleaner Production, vol. 88, no. 1, pp.297-307, 2015.

[8] H.P. Gupta, P.K. Tyagi, and M.P. Singh, "Regular node deployment for coverage in connected wireless networks," IEEE Sensors Journal, vo. 15, no. 12, pp.7126-7134, 2015.

[9] W. Li, C. Zhu, V.C. Leung, L.T. Yang, and Y. Ma, "Performance Comparison of Cognitive Radio Sensor Networks for Industrial IoT with Different Deployment Patterns," IEEE Systems Journal, vol. PP, no, 99, pp. 1-11, 2015.

[10] K. Sakai, M.T. Sun, W.S. Ku,T.H. Lai, and A.V. Vasilakos, "A Framework for the Optimal-Coverage Deployment Patterns of Wireless Sensors," IEEE Sensors Journal, vol. 15, no. 12, pp.7273-7283, 2015.

[11] K. Mukherjee, S. Gupta, A. Ray, and T.A. Wettergren, "Statistical-mechanics-inspired optimization of sensor field configuration for detection of mobile targets," IEEE Transactions on Systems, Man, and Cybernetics, Part B, vol. 41, no. 3, pp.783-791, 2011.

[12] S. Ivanov, K. Bhargava, and W. Donnelly, "Precision Farming: Sensor Analytics," IEEE Intelligent Systems, vol. 30, no. 4, pp.76-80, 2015.

[13] E. Onur, C. Ersoy, H. Deliç and L. Akarun, "Surveillance Wireless Sensor Networks: Deployment Quality Analysis," IEEE Network, vol. 21, no. 6, pp. 48-53, 2007.

[14] Z. Yun, X. Bai, D. Xuan, T. Lai & W. Jia, "Optimal Deployment Patterns for Full Coverage and K-Connectivity Wireless Sensor Networks," IEEE Transactions on Networking, vol. 18, no. 3, pp. 934-947, 2010.

[15] G. Stamenovic, S.R. Panic, D. Ranci, C. Stefanovi and M. Stefanovic "Performance analysis of wireless communication system in general fading environment subjected to shadowing and interference," EURASIP Journal on Wireless Communications, vol. 124, no. 1, pp. 1-8, 2014.

[16] X. Liu & M. Haenggi, "Throughput Analysis of Fading Sensor Networks with Regular and Random Topologies," EURASIP Journal on Wireless Communications and Networking, vol. 4, no. 1, pp. 554-564, 2005.

[17] R. Rajagopalan and P. K. Varshney, "Connectivity analysis of wireless sensor networks with regular topologies in the presence of fading," IEEE Trans. on Wireless Communications, vol. 8, no. 7, pp. 3475-3483, 2009.

[18] H. Wang, H. E. Roman, L. Yuan, Y. Huang and R. Wang, "Connectivity, coverage and power consumption in large-scale wireless sensor networks," Computer Networks, vol. 75, pp. 212-225, 2014.

[19] G. Fan, R. Wang, H. Huang, L. Sun and C. Sha, "Coverage-Guaranteed Sensor Node Deployment Strategies for Wireless Sensor Networks," Sensors, vol. 10, no. 3, pp. 2064-2087, 2010.

[20] Y. Chang, S. Zhang, Y. Zhang, J. Fan and J. Wang, "Uncertainty-Aware Sensor Deployment Strategy in Mixed Wireless Sensor Networks," International Journal of Distributed Sensor Networks, vol. 2013, no. 1, pp. 1-9, 2013.

[21] C. Zhu, C. Zheng and L. Shu, "A survey on coverage and connectivity issues in wireless sensor networks," Journal of Network and Computer Applications, vol. 35, no. 2, pp.619-632, 2012.

[22] M. Khalesian, and M.R. Delavar, "Wireless sensors deployment optimization using a constrained Pareto-based multi-objective evolutionary approach," Engineering Applications of Artificial Intelligence, vol. 53, no. 1, pp.126-139, 2016

[23] J. Chen, L. Zhang and Y. Kuo, "Coverage-Enhancing Algorithm Based on Overlap-Sense Ratio in Wireless Multimedia Sensor Networks," IEEE Sensors Journal, vol. 13, no. 6, pp. 2077-2083, 2013.

[24] 'INDRIYA': "Wireless Sensor Network Testbed, School of Computing, National University of Singapore", http://indriya.comp.nus.edu.sg/ Accessed on: 09/06/2016.

[25] S. He, J. Chen and Y. Sun, "Coverage and Connectivity in Duty-Cycled Wireless Sensor Networks for Event Monitoring," IEEE Transactions on Parallel and Distributed Systems, vol. 23, no. 3, pp. 475-482, 2012.

[26] C. He, J. Xing, J. Li, Q. Yang, R. Wang and X. Zhang, "A Combined Optimal Sensor Placement Strategy for the Structural Health Monitoring of Bridge Structures," International Journal of Distributed Sensor Networks, vol. 2013, no. 1, pp. 1-9, 2013.

[27] K. Ovsthus, and L. Kristensen, "An industrial perspective on wireless sensor networks a survey of requirements, protocols, and challenges," IEEE communications surveys & tutorials, vol. 16, no. 3, pp.1391-1412, 2014.

[28] C. T. Kone, A. Hafid and M. Boushaba, "Performance Management of IEEE 802.15.4 Wireless Sensor Network for Precision Agriculture," in IEEE Sensors Journal, vol. 15, no. 10, pp. 5734-5747, Oct. 2015.

[29] C. Lozoya, A. Aguilar and C. Mendoza, "Service Oriented Design Approach for a Precision Agriculture Datalogger," in IEEE Latin America Transactions, vol. 14, no. 4, pp. 1683-1688, April 2016.

[30] T.D. Le, and D.H. Tan, "Design and deploy a wireless sensor network for precision agriculture," In Proceedings on NICS, IEEE, pp. 294-299, Ho Chi Minh, Vietnam, September, 2015.

[31] C. Wang, D. George, and P.R. Green, P.R., "Development of plough-able RFID sensor network systems for precision agriculture," In Proceedings on WiSNET, IEEE, pp. 64-66, Newport Beach, CA USA, January 2014.

[32] J.H. Seok, J.Y. Lee, W. Kim, and J.J. Lee, "A bi-population-based evolutionary algorithm for solving full area coverage problems," IEEE Sensors Journal, vol. 13, no. 12, pp.4796-4807, 2013.

[33] A. S. Ibrahim, K. G. Seddik and K. R. Liu, "Connectivity-aware network maintenance and repair via relays deployment," IEEE Transactions on Wireless Communications, vol. 8, no. 1, pp. 356-366, 2009.

[34] K. He, M. Jia, and Q. Xu, "Optimal Sensor Deployment for Manufacturing Process Monitoring Based on Quantitative Cause-Effect Graph," IEEE Transactions on Automation Science and Engineering, vol. 13, no. 2, pp.963-975, 2016.

[35] A. Ababnah, and B. Natarajan, "Optimal control-based strategy for sensor deployment," IEEE Transactions on Systems, Man, and Cybernetics-Part A: Systems and Humans, vol. 41, no. 1, pp.97-104, 2011.

[36] J. Guo, and H. Jafarkhani, "Sensor Deployment with Limited Communication Range in Homogeneous and Heterogeneous Wireless Sensor Networks," IEEE Transactions on Wireless Communication, 2016 DOI 10.1109/TWC.2016.2590541

[37] O. Kaiwartya, S. Kumar, D.K. Lobiyal, P.K. Tiwari, A.H. Abdullah, and A.N. Hassan, "Multiobjective dynamic vehicle routing problem and time seed based solution using particle swarm optimization," Journal of Sensors, vol. 15, no.1, pp. 1-14, 2015.

Omprakash Kaiwartya received his Ph.D., degree in Computer Science from School of Computer and Systems Sciences, Jawaharlal Nehru University, New Delhi, India in 2015. He is currently a Postdoctoral Research Fellow at Faculty of Computing, Universiti Teknologi Malaysia (UTM), Johor Bahru, Malaysia. His research interests focus on Vehicular Ad-hoc Networks, Mobile Ad-hoc Networks and Wireless Sensor Networks.

Abdul Hanan Abdullah received his Ph.D. degree from Aston University in Birmingham, United Kingdom in 1995. He is currently working as a Professor at Faculty of Computing, Universiti Teknologi Malaysia, Johor Bahru, Malaysia. He was the dean at the faculty from 2004 to 2011. Currently he is heading Pervasive Computing Research Group, a research group under K-Economy Research Alliances. His research interests include Wireless Sensor Networks, Vehicular Adhoc Networks, Internet of Vehicles, Network Security and Next Generation Networks.

Yue Cao received his PhD degree from the Institute for Communication Systems (ICS) formerly known as Centre for Communication Systems Research, at University of Surrey, Guildford, UK in 2013. Further to his PhD study, he was a Research Fellow at the ICS. Since October 2016, he has been the Lecturer in Department of Computer Science and Digital Technologies, at Northumbria University, Newcastle upon Tyne, UK. His research interests focus on Delay/Disruption Tolerant Networks, Electric Vehicle (EV) charging management, Information Centric Networking (ICN), Device-to-Device (D2D) communication and Mobile Edge Computing (MEC).

Ram Shringar Raw received his Ph.D. degree in Computer Science from School of Computer and Systems Sciences, Jawaharlal Nehru University, New Delhi, India in 2011. He is currently working as Associate Professor at Department of Computer Science, Indira Gandhi National Tribal University, Amarkantak, India. His research interest includes Vehicular Ad-hoc Networks, Mobile Ad-hoc Networks and Wireless Sensor Networks.

Sushil Kumar received his Ph.D. degree in Computer Science from School of Computer and Systems Sciences, Jawaharlal Nehru University, New Delhi, India in 2014. He is currently working as Assistant Professor at School of Computer and Systems Sciences, Jawaharlal Nehru University, New Delhi, India. His research interest includes Vehicular Ad-hoc Networks, Mobile Ad-hoc Networks and Wireless Sensor Networks.

Xiulei Liu received the PhD degree in computer science from Beijing University of Posts and Telecommunications, P.R. China in March 2013. Since May 2013, he has been a Lecturer in Computer School, Beijing Information Science and Technology University, P.R. China. From October 2008 to October 2010, he was a visiting PhD student in Centre for Communication System Research (CCSR), University of Surrey, UK. His research interests include semantic sensor, semantic web, knowledge graph, semantic information retrieval.

Rajiv Ratn Shah received his M. Tech. from Delhi Technological University, New Delhi, India in 2012. He is currently a PhD candidate in School of Computing, National University of Singapore (NUS), Singapore. His main research interests focus on multimodal analysis of user-generated content in support of social media applications, location-based services in support of social media applications, multimedia analysis and retrieval.